Superior Electrochemical Performances of Highly Porous Bismuth Oxyhalide [BiOX (X = Br, Cl, I)]/Lemon Peel Derived Activated Carbon Electrode Materials for Solid State Asymmetric and Symmetric Supercapattery Devices

Junaid Khan[a, b] **, Anique Ahmed[c], Abdullah A. Al-Kahtani[d]

[a]Department of Physics, Government Postgraduate Collage No.1, Abbottabad, Khyber Pakhtunkhwa, Pakistan

[b]Department Of Higher Education Achieves and Libraries, Government of Khyber Pakhtunkhwa, Pakistan

[c]Ghulam Ishaq Khan Institute of Engineering Sciences and Technology Topi, Khyber Pakhtunkhwa Pakistan

[d]Chemistry Department, Collage of Science, King Saud University, P. O. Box 2455, Riyadh-22451, Saudi Arabia

**Email: junaidkhan.nanotech@gmail.com

1.1. Materials

Bismuth Nitrate Pentahydrate ($Bi(NO_3)_{3.5}H_2O$), Potassium Chloride (KCl), Potassium Iodide (KI), Glacial Acetic Acid (CH_3COOH), Hydrochloric Acid (HCl), Polyvinyl Alcohol (PVA) and Potassium Hydroxide (KOH) were received from Merck. Carbon Black and Poly - 1,1 - difluoroethene (PVDF) were purchased from Alfa Aesar. N-Methyl Pyrrolidone (NMP, 99%) and Potassium Bromide (KBr) were obtained from Sigma Aldrich. All these chemicals were used without any further purification and Double - Distilled (DD) water was used throughout the study.

1.2. Characterization

The crystallinity and average crystallite size of the prepared BB, BC, BI, LPAC, BBAC, BCAC and BIAC were studied using Bruker Advanced-D8 Powder X-ray Diffractometer equipped with Accelerator detector (Cu -Kα radiation, λ=1.5418 Å). The characteristic vibrations of the synthesized samples were analyzed using Perkin Elmer Fourier Transform Infrared spectrometer (attenuated total reflection mode) in the wavenumber range of 400 cm−1 – 4000 cm−1. The morphology and chemical compositions of the prepared samples were characterized by Field Emission Scanning Electron Microscope (FESEM: ZEISS Sigma) with Energy-Dispersive X-ray Spectroscopy studies. The structural characteristics of the prepared samples were examined using High-Resolution Transmission Electron Microscopy (HRTEM: FEI Tecnai G2 20 S-TWIN) with an accelerating voltage of 200kV. Further, the surface area and porosity of the prepared materials were studied using Nitrogen Gas Adsorption-Desorption Isotherm analysis by Brauner-Emmet-Teller (BET) and Barrett-Joyner-Halenda (BJH) (Model Autosorb IQ, Quantachrome Instruments)

methods respectively. Thermogravimetric Analysis (TGA) was carried out in the temperature range of 30°C - 900°C at a heating rate of 10°C/min using Netszch (STA ff3 Jupiter) to analyze the thermal properties of the prepared samples.

The electrochemical performance of the prepared BB, BC, BI, LPAC, BBAC, BCAC and BIAC was analyzed by Cyclic Voltammetry (CV), Chronopotentiometry and Electrochemical Impedance analysis (EIS) using CHI608E electrochemical workstation. where three electrode cell configuration was adopted. In the present work, 1 M aqueous KOH as electrolyte, prepared nanomaterials with PVDF binder and carbon black as working electrode, Ag/AgCl as reference electrode and Platinum wire (Pt) as counter electrode were used in this configuration. The preparation of working electrode is as follows: A 80% of prepared nanomaterials, 10% of carbon black and 10% of PVDF binder were mixed together with a few drops of N-Methylpyrrolidone (NMP) solvent. Then the obtained slurry was coated on Ni foam (area of 1×1 cm^2) and dried at 60°C in an oven for overnight. In the electrochemical studies, the potential is applied between working and reference electrodes and the current is measured between working and counter electrodes. The performance of both symmetric [(BiOBr/LPAC)||(BiOBr/LPAC)] and asymmetric [(BiOBr/LPAC)||(LPAC)] solid state supercapattery devices was tested in a two electrode configuration. In the symmetric solid state supercapattery device, the prepared BBAC (BiOBr/LPAC) nanocomposite was utilized as both positive and negative electrodes. But in the case of asymmetric solid state supercapattery device, the BBAC (BiOBr/LPAC) nanocomposite was served as positive electrode and LPAC nanomaterial was used as negative electrode where PVA/KOH was used as solid electrolyte.

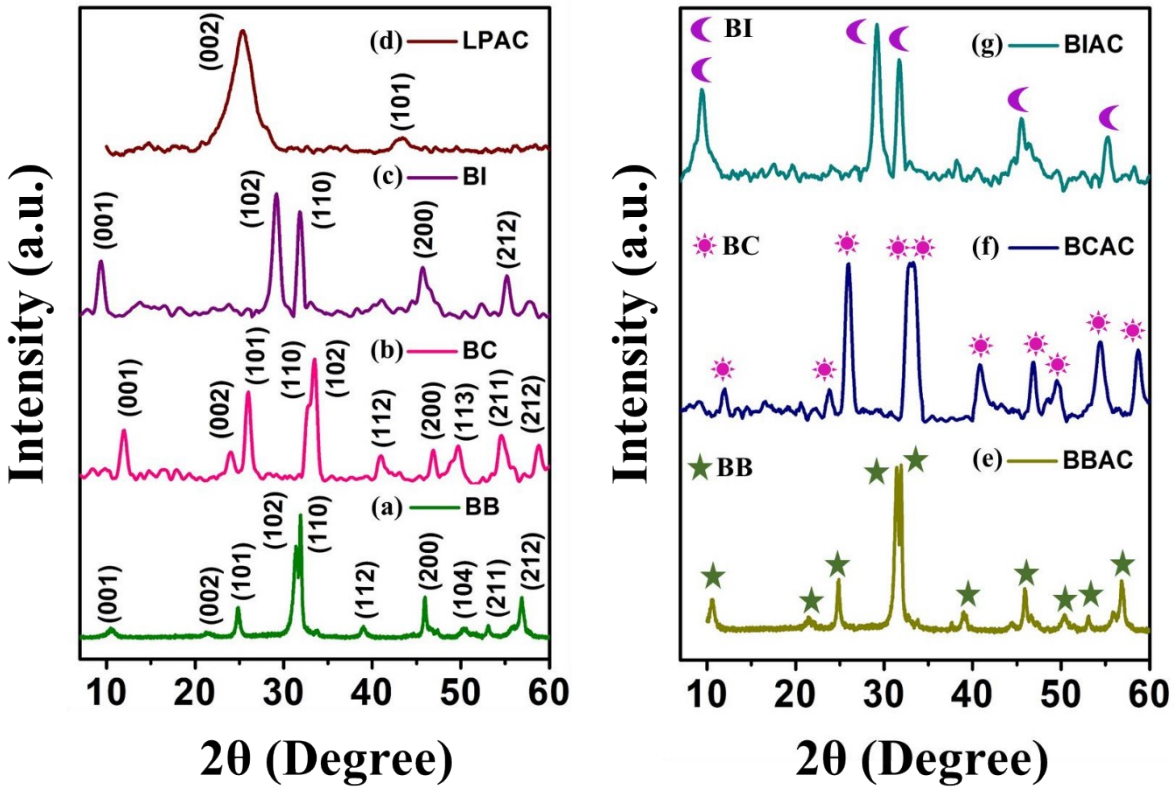

Fig. S1. XRD pattern of prepared (a) BB, (b) BC, (c) BI, (d) LPAC, (e) BBAC, (f) BCAC and (g) BIAC electrode materials

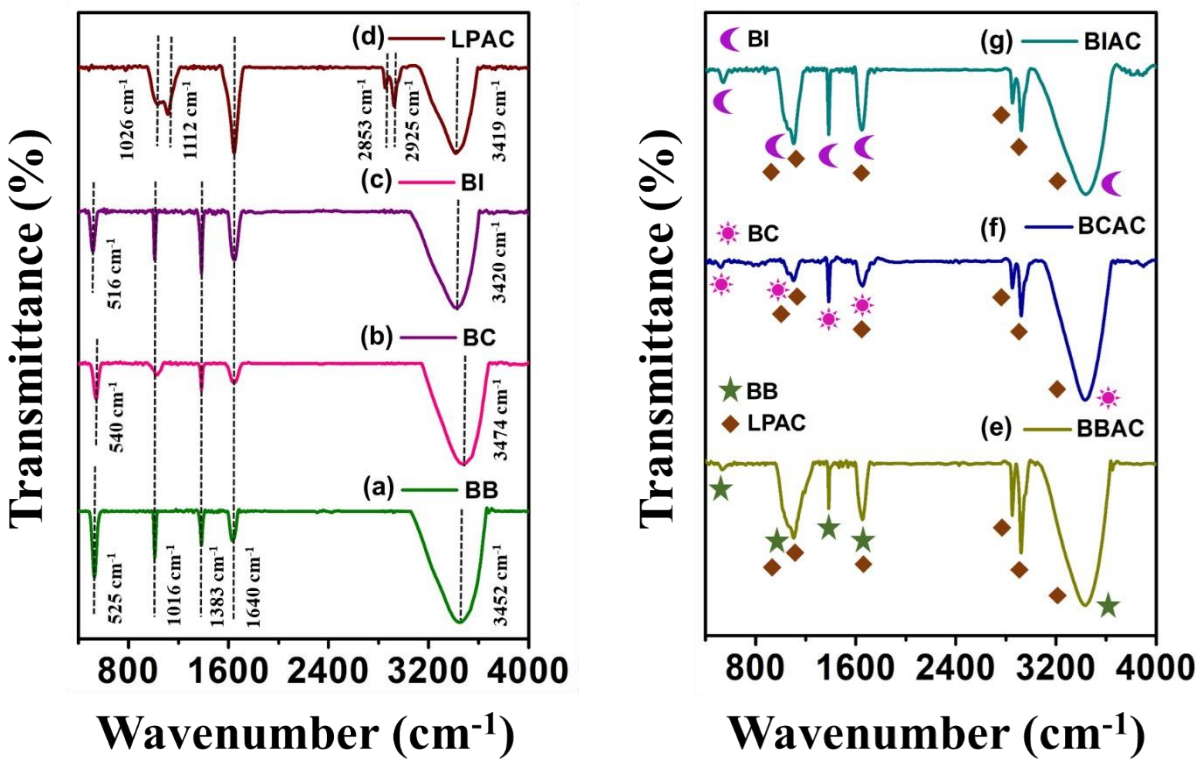

Fig. S2. FTIR spectrum of prepared (a) BB, (b) BC, (c) BI, (d) LPAC, (e) BBAC, (f) BCAC and (g) BIAC electrode materials

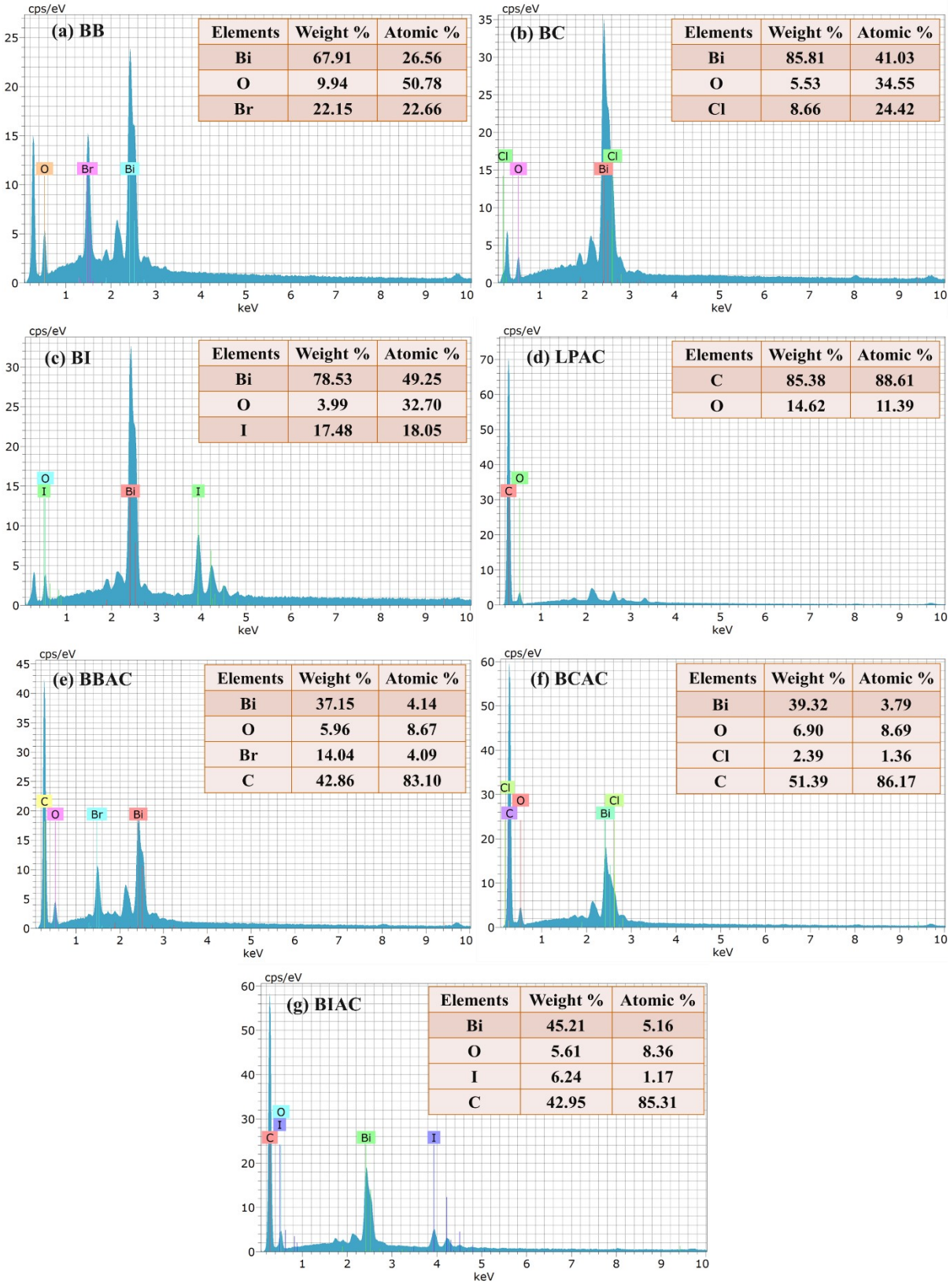
(a) BB
cps/eV
keV
O
Br
Bi
Elements | Weight % | Atomic %
Bi | 67.91 | 26.56
O | 9.94 | 50.78
Br | 22.15 | 22.66
(b) BC
cps/eV
keV
Cl
O
Bi
Cl
Elements | Weight % | Atomic %
Bi | 85.81 | 41.03
O | 5.53 | 34.55
Cl | 8.66 | 24.42
(c) BI
cps/eV
keV
O
I
Bi
I
Elements | Weight % | Atomic %
Bi | 78.53 | 49.25
O | 3.99 | 32.70
I | 17.48 | 18.05
(d) LPAC
cps/eV
keV
O
C
Elements | Weight % | Atomic %
C | 85.38 | 88.61
O | 14.62 | 11.39
(e) BBAC
cps/eV
keV
C
O
Br
Bi
Elements | Weight % | Atomic %
Bi | 37.15 | 4.14
O | 5.96 | 8.67
Br | 14.04 | 4.09
C | 42.86 | 83.10
(f) BCAC
cps/eV
keV
Cl
O
C
Cl
Bi
Elements | Weight % | Atomic %
Bi | 39.32 | 3.79
O | 6.90 | 8.69
Cl | 2.39 | 1.36
C | 51.39 | 86.17
(g) BIAC
cps/eV
keV
O
I
C
Bi
I
Elements | Weight % | Atomic %
Bi | 45.21 | 5.16
O | 5.61 | 8.36
I | 6.24 | 1.17
C | 42.95 | 85.31

Fig. S3. EDAX spectra of (a) BB, (b) BC, (c) BI, (d) LPAC, (e) BBAC, (f) BCAC and (g) BIAC electrode materials

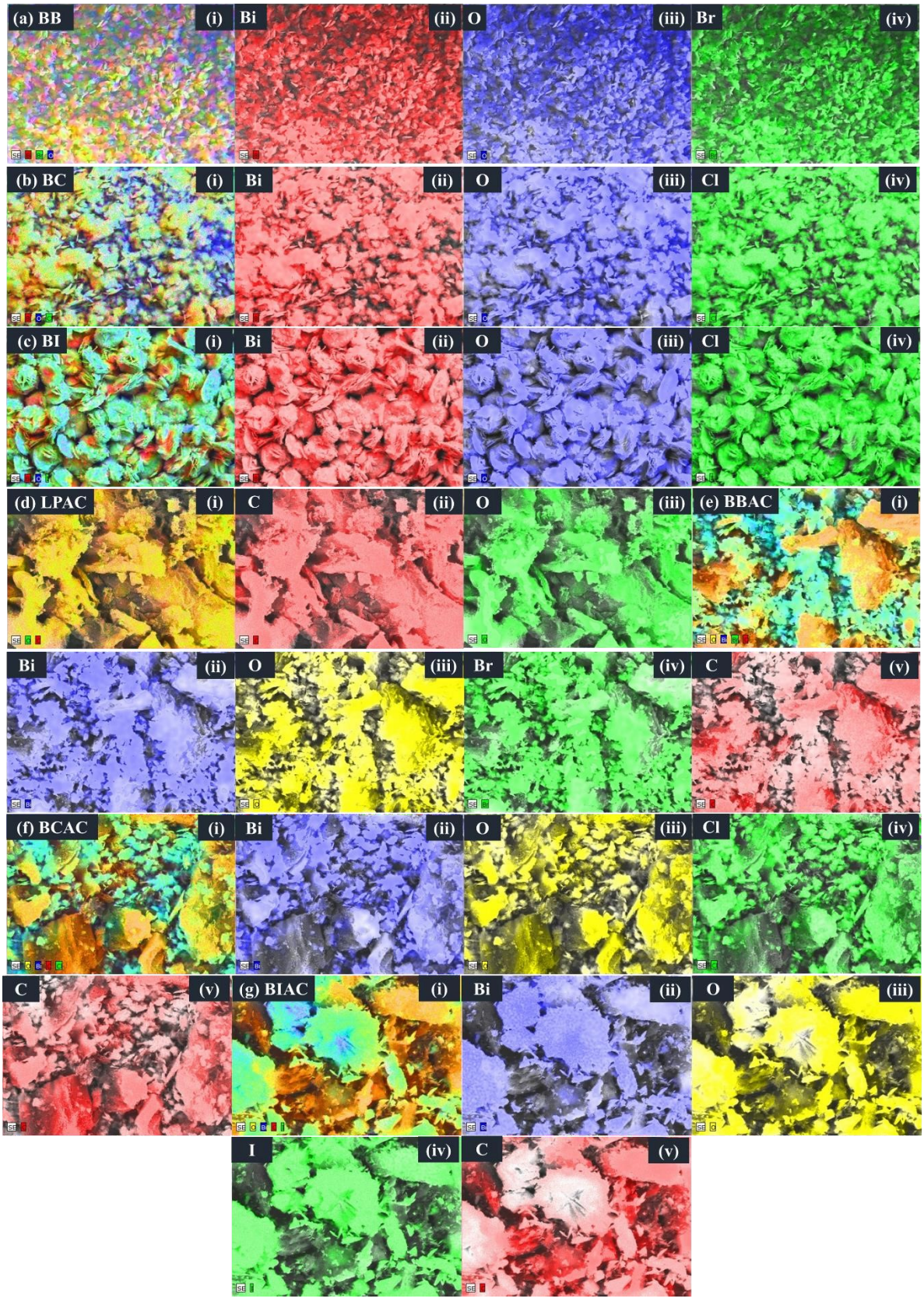
(a) BB
(i)
Bi
(ii)
O
(iii)
Br
(iv)
(b) BC
(i)
Bi
(ii)
O
(iii)
Cl
(iv)
(c) BI
(i)
Bi
(ii)
O
(iii)
Cl
(iv)
(d) LPAC
(i)
C
(ii)
O
(iii)
(e) BBAC
(i)
Bi
(ii)
O
(iii)
Br
(iv)
C
(v)
(f) BCAC
(i)
Bi
(ii)
O
(iii)
Cl
(iv)
C
(v)
(g) BIAC
(i)
Bi
(ii)
O
(iii)
I
(iv)
C
(v)

Fig. S4. Elemental mapping of (a) BB, (b) BC, (c) BI, (d) LPAC, (e) BBAC, (f) BCAC and (g) BIAC electrode materials

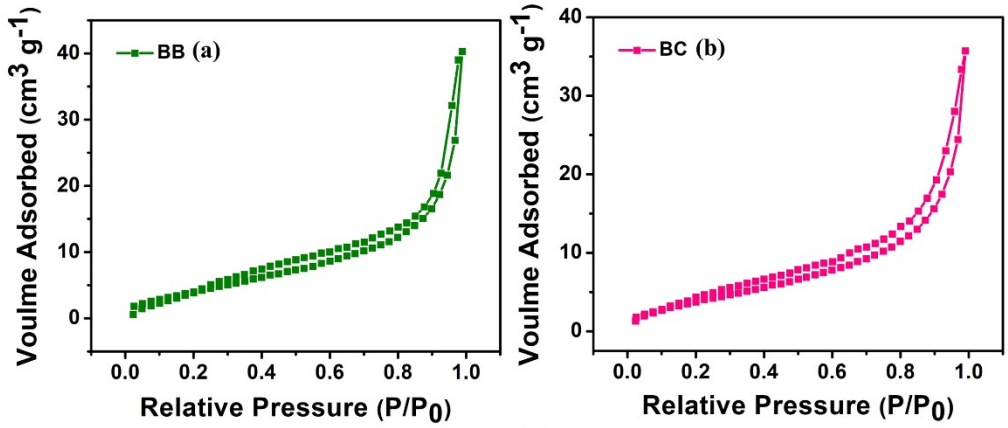
BB (a)
Voulme Adsorbed (cm3 g-1)
Relative Pressure (P/P0)

BC (b)
Voulme Adsorbed (cm3 g-1)
Relative Pressure (P/P0)

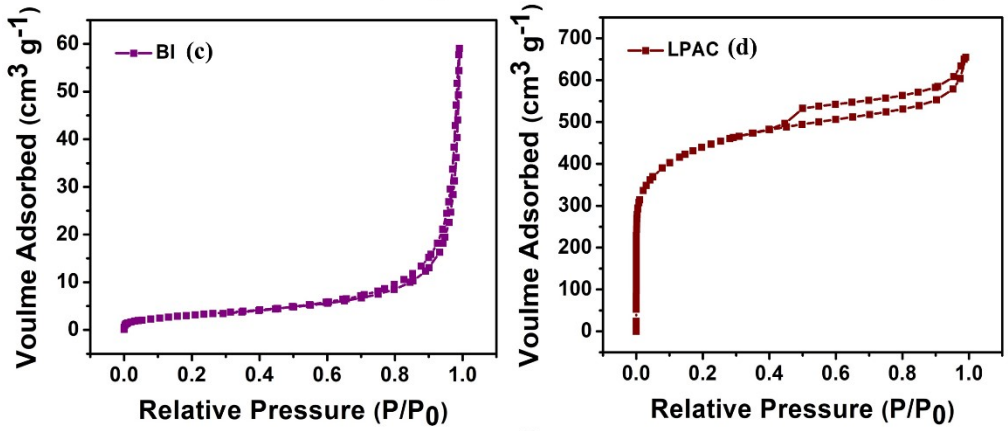
BI (c)
Voulme Adsorbed (cm3 g-1)
Relative Pressure (P/P0)

LPAC (d)
Voulme Adsorbed (cm3 g-1)
Relative Pressure (P/P0)

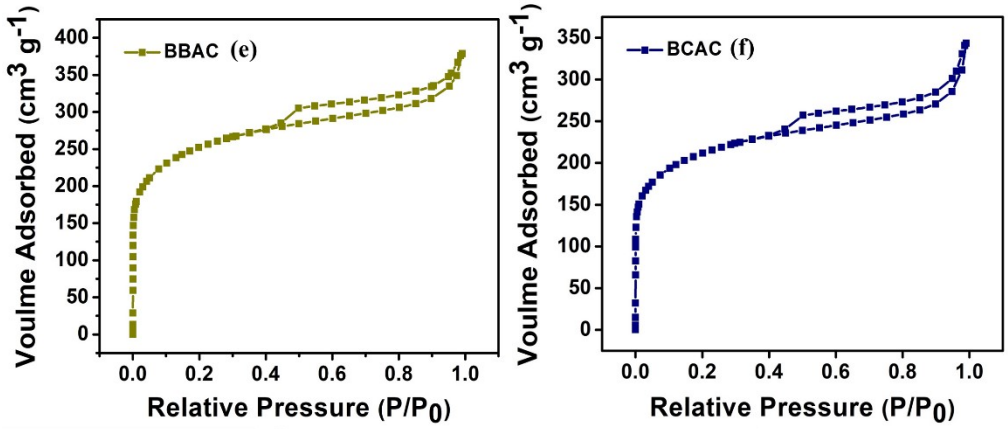
BBAC (e)
Voulme Adsorbed (cm3 g-1)
Relative Pressure (P/P0)

BCAC (f)
Voulme Adsorbed (cm3 g-1)
Relative Pressure (P/P0)

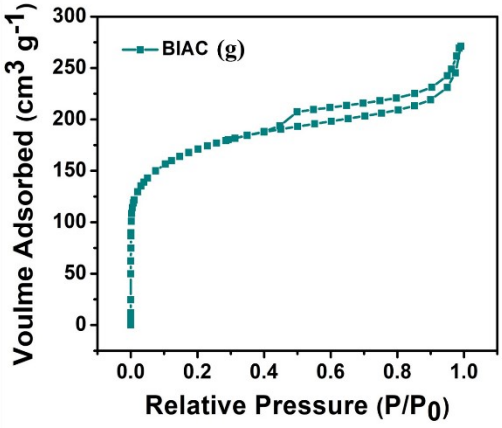
BIAC (g)
Voulme Adsorbed (cm3 g-1)
Relative Pressure (P/P0)

Fig. S5. BET analysis of (a) BB, (b) BC, (c) BI, (d) LPAC, (e) BBAC, (f) BCAC and (g) BIAC electrode materials

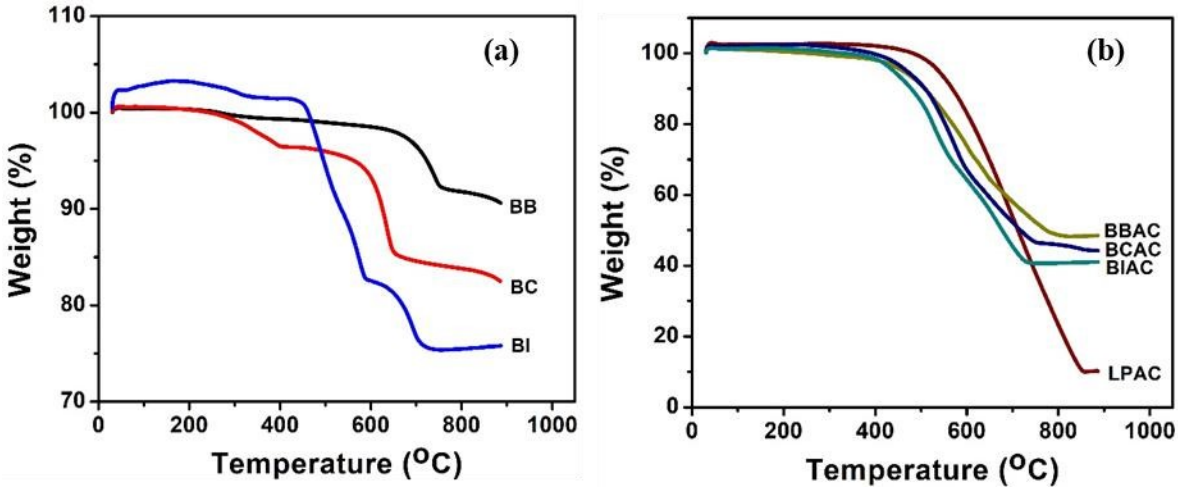

Fig. S6. TGA curve of (a) BB, BC, BI and (b) LPAC, BBAC, BCAC, BIAC Electrode Materials.

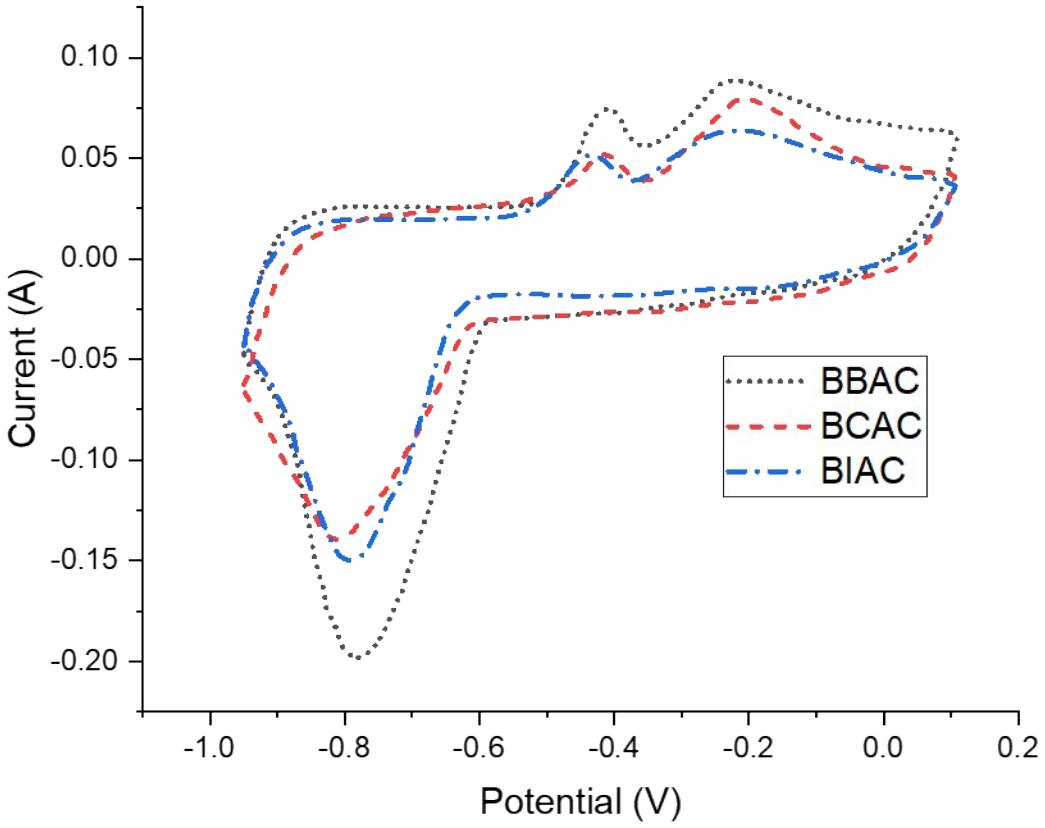

Fig. S7. Comparison of CV profiles of BBAC, BCAC, and BIAC recorded at 10 mV/s.

1.3. LED operation with fabricated device

To examine the prepared solid state asymmetric (BiOBr/LPAC||LPAC) and symmetric (BiOBr/LPAC||BiOBr/LPAC) supercapattery devices for practical applications, both devices ASC and SSC were charged for 1 min. The asymmetric solid state supercapattery device (BiOBr/LPAC||LPAC) could light up a commercial red LED for 7 min 18 s (438 s) (see Fig. 14(a-f)) and the same could power an electric motor fan for 1 min 31 s (91 s) (see Fig 15(a-f)). whereas, the symmetric solid state supercapattery device (BiOBr/LPAC||BiOBr/LPAC) could light up a commercial red LED for 9 min 15 s (555 s) (see Fig. 16(a-f)) and an electric motor fan for 2 min 2 s (122 s) (see Fig 17(a-f)). From these results, it is observed that the prepared solid state symmetric (BiOBr/LPAC||BiOBr/LPAC) supercapattery device offers superior electrochemical performance than solid state asymmetric (BiOBr/LPAC||LPAC) supercapattery device. Hence, the prepared BiOBr/LPAC||BiOBr/LPAC solid state symmetric supercapattery device with high operating potential (2.6 V), outstanding energy density (172.06 Wh/kg) and excellent power density (6.5 kW/kg) may act as a potential power source.

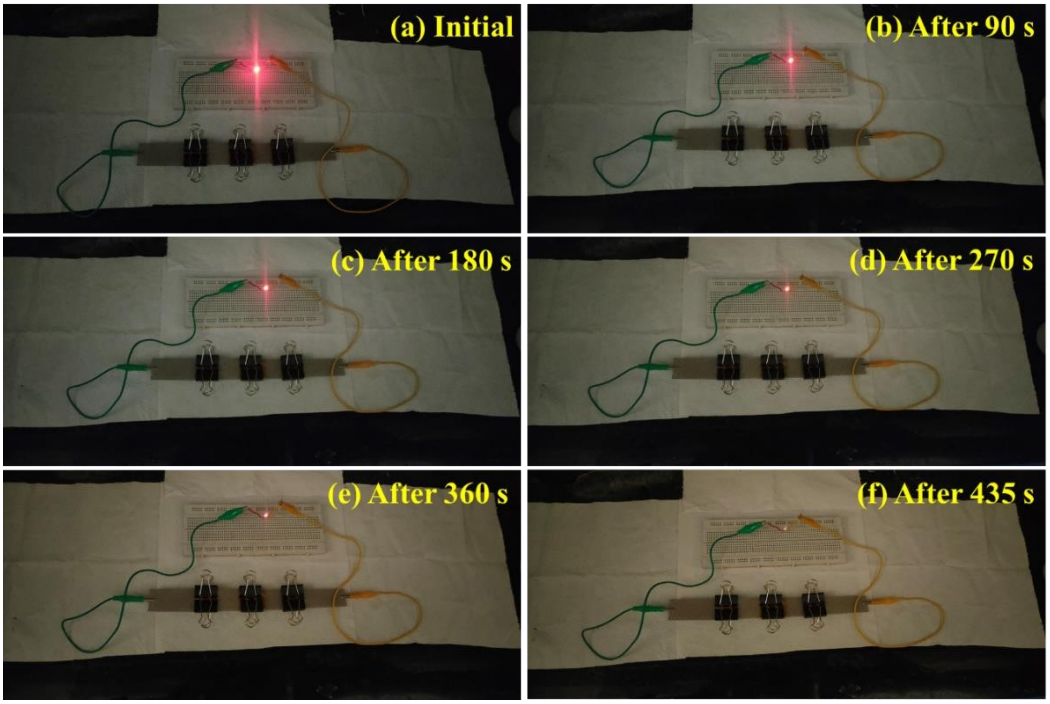

Fig. S8. Photographs of (a–f) two serially connected solid state asymmetric supercapattery device (BiOBr/LPAC||LPAC) light up a red LED during 435 s. (For interpretation of the references to colour in this figure legend, the reader is referred to the web version of this article)

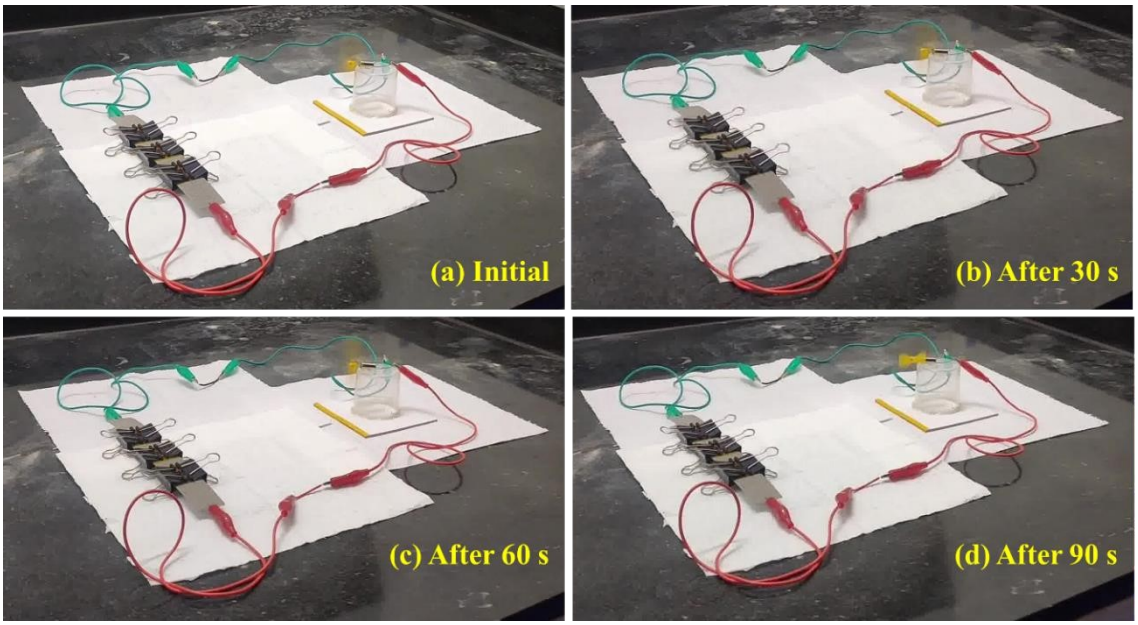

Fig. S9. Photographs of (a–d) two serially connected solid state asymmetric supercapattery device (BiOBr/LPAC|| LPAC) powering an electrical motor fan (3.7 V) during 90 s

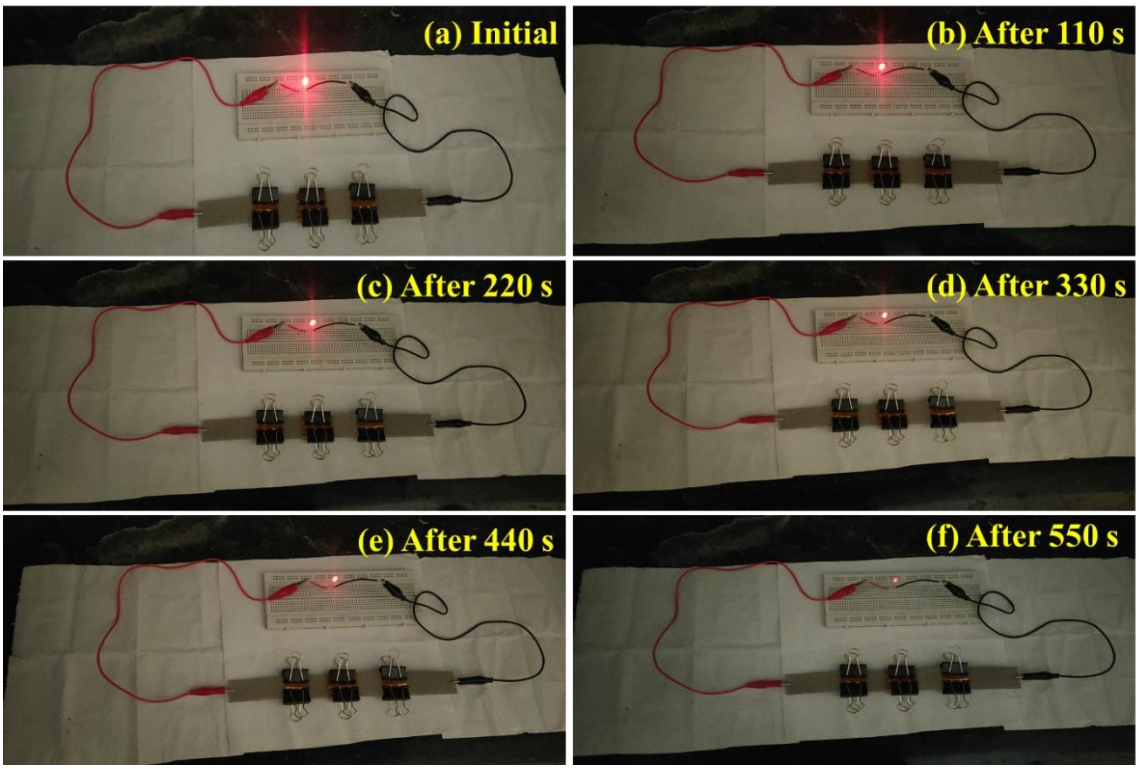

Fig. S10. Photographs of (a-f) two serially connected solid state symmetric supercapattery device (BiOBr/LPAC|| BiOBr/LPAC) light up a red LED during 550 s. (For interpretation of the references to colour in this figure legend, the reader is referred to the web version of this article)

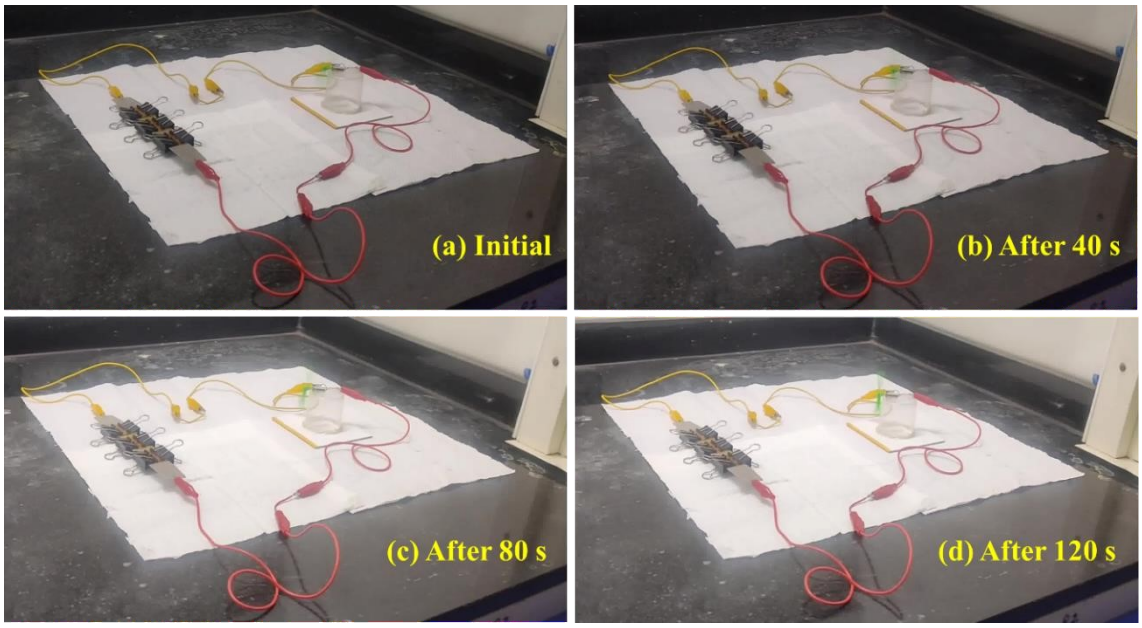

Fig. S11. Photographs of (a–d) two serially connected solid state symmetric supercapattery 22 device (BiOBr/LPAC||BiOBr/LPAC) powering an electrical motor fan (3.7 V) during 120 s

Table S1. Crystallographic properties of the prepared electrode materials

Prepared Electrode Materials	Grain Size (nm)	Crystallinity (%)
BB	12.96	93.76
BC	13.78	89.93
BI	14.55	71.61
LPAC	4.67	59.94
BBAC	11.03	77.38
BCAC	11.34	75.91
BIAC	11.87	63.41

Table S2. Distance and angle between the nearest diffraction spots of the prepared BB, BC, and BI electrode materials

Parameters	BB	BC	BI
Distance (nm^{-1}) r_1	3.58	3.69	3.55
Distance (nm^{-1}) r_2	5.27	5.21	5.19
Angle (°) θ	45°	45°	45°

Table S3. Specific surface area, pore volume, and pore size of the prepared electrode materials

Electrode Materials	Specific Surface Area (m^2/g)	Pore Volume (cm^3/g)	Pore Size (nm)
BB	18.19	0.061	2.98
BC	16.12	0.054	3.32
BI	11.80	0.087	2.94
LPAC	1610	1.010	2.52
BBAC	981	0.583	2.38
BCAC	783	0.529	2.70
BIAC	610	0.418	2.74

Table S4. Decomposition temperature (°C) and weight loss (%) of the prepared BB, BC, BI, LPAC, BBAC, BCAC, and BIAC electrode materials

Electrode Materials	Decomposition Temperature (°C)	Weight Loss (%)
BB	667	9.38
BC	562	17.52
BI	448	24.19
LPAC	495	89.79
BBAC	442	51.50
BCAC	436	55.77
BIAC	413	58.94

Table S5. Anodic and cathodic peaks of the prepared BB, BC, and BI electrodes

Electrodes	**Anodic Peaks (V)**	**Cathodic Peak (V)**
	O_1	**O_2**
BB	−0.52	−0.31
BC	−0.48	−0.27
BI	−0.59	−0.39

Table S6. Electrochemical resistance parameters of the prepared electrode materials

Electrode Materials	**Rs (Ω)**	**Rct (Ω)**
BB	1.27	3.67
BC	1.37	3.87
BI	1.50	4.38
LPAC	1.01	2.83
BBAC	0.63	2.12
BCAC	0.72	2.33
BIAC	0.87	2.60